

Moving boulders in flash floods and estimating flow conditions using boulders in ancient deposits

JAN ALEXANDER* and MARK J. COOKER†

*School of Environmental Sciences, University of East Anglia, Norwich Research Park, Norwich, NR4 7TJ, UK (E-mail: j.alexander@uea.ac.uk)

†School of Mathematics, University of East Anglia, Norwich Research Park, Norwich, NR4 7TJ, UK

Associate Editor – Vern Manville

ABSTRACT

Boulders moving in flash floods cause considerable damage and casualties. More and bigger boulders move in flash floods than predicted from published theory. The interpretation of flow conditions from the size of large particles within flash flood deposits has, until now, generally assumed that the velocity (or discharge) is unchanging in time (i.e. flow is steady), or changes instantaneously between periods of constant conditions. Standard practice is to apply theories developed for steady flow conditions to flash floods, which are however inherently very unsteady flows. This is likely to lead to overestimates of peak flow velocity (or discharge). Flash floods are characterised by extremely rapid variations in flow that generate significant transient forces in addition to the mean-flow drag. These transient forces, generated by rapid velocity changes, are generally ignored in published theories, but they are briefly so large that they could initiate the motion of boulders. This paper develops a theory for the initiation of boulder movement due to the additional *impulsive force* generated by unsteady flow, and discusses the implications.

Keywords Boulders, flash floods, flood front, hydrodynamic impact, palaeohydrology.

INTRODUCTION

The phrase ‘flash flood’ is used widely to refer to inundation resulting from intense short precipitation events (Archer & Fowler, 2015). However, there is no universal definition of ‘flash flood’, and very similar events due to failure of natural or artificial dams, levées or embankments (e.g. Spinewine & Zech, 2007; Zech & Soares-Frazão, 2007; Bohorquez, 2008), subglacial outburst and disruption of ice jams (e.g. Jasek, 2003) may also be called flash floods. Most types of lahar (floods related to volcanic activity and entraining volcanoclastic material; Vallance, 2000) may also be classed as flash floods, and result from differing triggering mechanisms (e.g. Cronin *et al.*, 1997; Barclay *et al.*, 2007; Kilgour *et al.*, 2010).

Flash flood is here defined as any overland flow of water (within or outside a river channel)

that arrives suddenly at a fixed point, changes quickly and lasts a short time; thus, they are inherently unsteady (velocity at any fixed point in space varying over time) and non-uniform (velocity varying in space at one time). The water depth is also time dependant. The flow develops and fluctuates on many time scales, from surface splashes started in less than one second, to the head of the flash flood passing in seconds or minutes, to the complete passage of the flood in minutes or hours. A flash flood is depicted schematically in Fig. 1 to illustrate the component parts as referred to in this paper. The first arrivals of flash floods (the flood fronts) are commonly reported as a ‘wall of water’ (e.g. Hjalmarsen, 1984; Archer & Fowler, 2015), with high sediment or debris load that may cause catastrophic damage and risk to life (for example, see video clips at <http://www.youtube.com/>

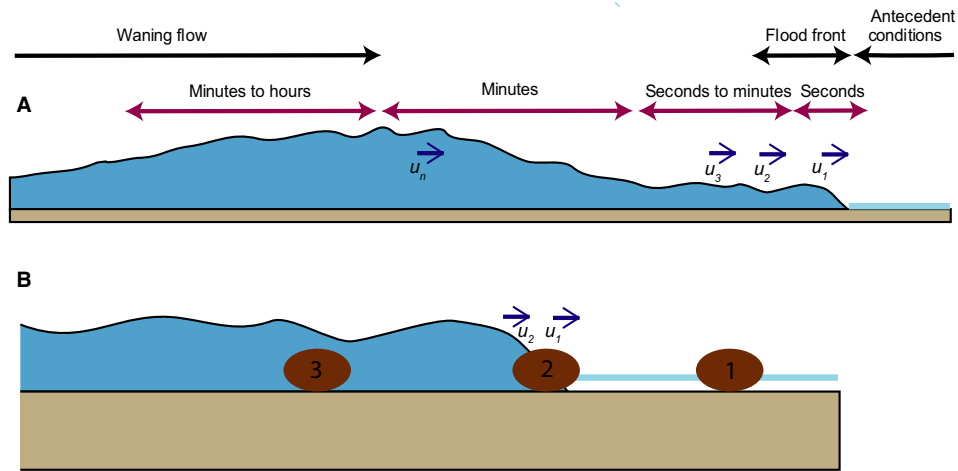


Fig. 1. (A) A schematic sketch of the passage of a flow to show the critical features of a flash flood. In this schematic, time at a fixed observation point increases from right to left. The components of the diagram are not drawn at the same horizontal scale. There may or may not be some flow before arrival of the flood front. Depending on conditions, the trailing zone may or may not be wave trains. Symbols refer to conditions discussed later in the text. (B) Illustration of transient conditions acting on a boulder on the bed. Boulder 1 is in a static state with little or no flow, before the flash flood front arrives. The flood front at Boulder 2 is causing very rapid change in conditions and a strong impulsive force. After the front has passed, the forces on the boulder might be expected to decline, but the velocity fluctuation continues to supply impulsive forces on Boulder 3.

watch?v=TDtBby7lJX0). In many sites the flood front may be steep (especially for flows with high solids-content) and associated with very rapid changes in conditions. The discharge can continue to increase for some time after the passage of the flood front (defined in the sketch of the full passage of a flow in Fig. 1A). The transience of flood fronts not only explains their impact but also the paucity of photographic records and scientific study. During a flood, inherent instability in the flow may lead to the development of a surge (flood bore) or multiple surges (e.g. Cornish, 1910; Jeffreys, 1925; Weir, 1982; Vignaux & Weir, 1990; Lube *et al.*, 2012). In sediment-laden floods these have similarities to the surges developed in debris flows (cf. Zanuttigh & Lamberti, 2007). Flash floods may be clear water flows, or may entrain large volumes of sediment to become concentrated or hyperconcentrated flows (cf. Mulder & Alexander, 2001) and may change locally or temporarily into debris flows. Because of the potential for rapid sediment entrainment and deposition, the sediment concentration, and thus bulk density of parts of the flow, may change rapidly in time or space.

This paper considers boulder movement in flash floods where rapidly changing flow conditions occur at the flood front or during passage of subsequent bores or surges. The theory is

applicable to a range of conditions from clear stream flow to hyperconcentrated flow. Not only will the local velocity and depth vary in such flows, but also the suspended sediment concentration, and thus bulk density of the fluid, because of feedback with the bed and variations in sediment availability (cf. Malmon *et al.*, 2007; Alexander *et al.*, 2010). Some of the modelling presented in this article may be applicable to debris flows also, but in those flows other factors, such as local pore pressure changes and flow yield strength (cf. Iverson, 1997), may have a major influence on boulder mobility.

Particle size of deposits has frequently been used to estimate the flow conditions at the time of deposition (e.g. Komar, 1989; Clarke, 1996). Many flash flood deposits contain boulders of considerable size, relative to the depth of the flow that transported them (Fig. 2). In palaeoflood hydrology the largest boulders in a deposit may be used to infer the palaeoflow velocity (Costa, 1983; Komar, 1987; Clarke, 1996; Mather & Hartley, 2005). Costa (1983), Clarke (1996), O'Connor (1993) and others attempt to calculate the minimum critical force needed to move a boulder of a given size. These established methodologies are likely to overestimate the flow velocity, because not all of the forces acting on the boulder in a flash flood are taken into account. There are numerous possible sources of error in the esti-

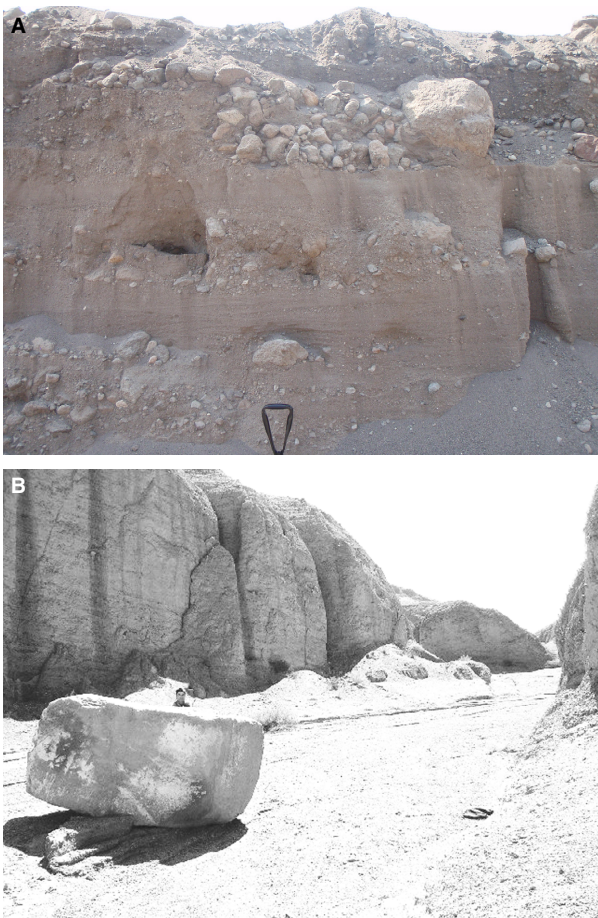


Fig. 2. (A) Photograph of boulders in a lahar deposit in the Belham Valley on the Caribbean island of Montserrat (photograph by Melanie Froude, University of East Anglia). The vertical section was excavated mechanically into sediments that were deposited by lahars (volcanic sediment-laden flash flood) on 13 to 14 October 2012 (Froude *et al.*, 2013). The flow was diagonally out of the face towards the right of the photographer. The large boulder towards the top of the section has a diameter of *ca* 0.5 m and large boulders are present elsewhere in this deposit. (B) Photograph from Anne Mather (Plymouth University) of boulder deposited from a flow event on the hyper-arid Arcas alluvial fan, Atacama, northern Chile. In both of these examples the flow depth is likely to have peaked at little more than the boulder diameter, and the suspended sediment concentration could have been high, but there is no evidence of debris flow behaviour.

mates of boulder movement initiation conditions, including: bed roughness and form drag (e.g. Petit *et al.*, 2005); emergence (e.g. Shvidchenko & Pender, 2000; Carling *et al.*, 2002a); suspended sediment concentration (e.g. Billi, 2011); grain packing and sorting (e.g. Laronne & Carson, 1976; Church, 1978); individual grain exposure (e.g.

Andrews, 1983; Church *et al.*, 1998; Carling *et al.*, 2002b); sediment types available for transport (Bridge & Bennett, 1992); clast and fluid density (Clarke, 1996); and slope (e.g. Meirovich *et al.*, 1998; Parker *et al.*, 2011). Near-bed turbulent velocity fluctuations have been considered to give momentary tractive forces two to four times greater than average values (Graf, 1971). The maximum excursions of velocity from the average velocity in a flow depend on the Reynolds number Re and in most natural water flows Re is so large (10^5 or more) that the flow is fully turbulent. This is the case for flash floods, except when they entrain so much sediment that they become hyperconcentrated and behave as non-Newtonian fluids. For a flow with a time-averaged velocity of u_0 the turbulence admits flow speeds as low as zero and as high as $2u_0$ or more (McComb, 1990). The sudden arrival of a flash flood front at a boulder means that the velocity rises from zero (or near zero if there is some antecedent flow) to u_0 with additional turbulent fluctuations (Fig. 1).

Computational fluid dynamics of time-dependent flows has been successfully applied to modelling outburst floods (e.g. Komatsu *et al.*, 2009; Alho *et al.*, 2010), jökulhlaups (Carrivick, 2007) and lahars (Carrivick *et al.*, 2009), but the outputs of these need to be compared with field data on geomorphological features and deposit structures and grain size, to assess the modelled flow conditions (Carrivick *et al.*, 2010). Geographic Information System (GIS) based inundation models, such as LAHARZ have been used to estimate flow speeds and inundation depths in lahar risk sites, such as on the Caribbean Island of Montserrat (Darnell *et al.*, 2013). All of these approaches are limited to use in recent or geologically very young events by a requirement for quantified pre-flow topography. Further difficulties arise because of poor knowledge of syn-flow erosion, changing flow rheology with sediment bulking and debulking, and assumptions about water volume or flux. Increased understanding of boulder entrainment and transport in unsteady flows is needed to improve the reliability of these models. Established methods for finding the critical conditions for movement of particles on a bed (e.g. Costa, 1983; Williams, 1983; Ferguson, 2005) based on a dimensionless critical shear stress (Shields parameter), near-bed velocity or bedload estimates based on stream power, all generally assume that the velocity (or discharge) is unchanging in time. When conditions change, either time-averaged conditions or short periods of constant

conditions are considered, not the change itself. However, the fact that the velocity or other factors are different at different times during a flash flood may be far less important than the change itself, especially when that change is rapid or sudden. In flash floods, the arrival of a flood bore and the onset of particle movement may be almost instantaneous (Reid *et al.*, 1998). The rapidity of change, and the special conditions of forces associated with the time-dependence, have been ignored previously. Thus, established methods that consider boulder size can lead to: (i) underestimates of clast size; (ii) underestimates of the volume of sediment in motion in a flash flood; or (iii) overestimates of the velocity or discharge based on deposited boulder size.

The incomplete consideration of forces acting on a boulder has implications for interpretation of ancient deposits, and has consequences for the nature of the hazard in flash floods. A greater number of bigger clasts, and notably boulders, are more mobile in flash floods than expected, either intuitively or from steady-flow theory for a given flow speed and depth. This hypothesis comes from current observations of flash floods in many climatic and geographic settings, news reports and video records. Further fluid-dynamical consideration of forces due to rapidly changing water velocity in sea waves (Cooker & Peregrine, 1995; Cox & Cooker, 1999) has shown that large boulders can be moved by breaking waves of modest height.

THE UNSTEADINESS OF FLOW WITHIN A FLASH FLOOD

Unsteadiness occurs on a wide range of scales within a flash flood. The arrival of the flood front may change from little or no flow to a lot of flow in seconds (Fig. 1). Turbulent fluctuations (producing bursts and sweeps) occur throughout each event (where not suppressed by high sediment concentrations) but most of these have length scales much smaller than boulder diameter (in turbulence, length scales of velocity tend to shorten over time) and do not contribute to the model presented below. However, those velocity fluctuations that occur on the length scale of a boulder play a significant role in the instantaneous hydrodynamic forces acting on it. In addition, in many flash floods, because the flows may be rapid, trains of stationary waves (associated with antidunes) may form (cf. Froude, 2015). These waves may break in isolation or groups of

waves in trains may break synchronously producing surges (both upstream and downstream) that entrain sediment (Fahnestock & Haushild, 1962). Flood bores formed by this mechanism or others generate quick variations in conditions. There may be many such bores within a flash flood (Froude, 2015, recorded 349 bores in two days in a flash flood on Montserrat in the Caribbean. Bores were observed at 6 to 6002 sec intervals during peak flow).

It is inherently difficult to measure flow properties of flash floods. Despite this there are some published records that illustrate the nature of the rapid variations. For example, Doyle *et al.* (2011) observed eight rain-triggered flash floods (lahars) on Semeru Volcano, East Java, in which bulking (entrainment of sediment and water) and debulking (dilution and sedimentation) occurred. Each lahar lasted from 1 to 3 h with flow depths of 0.5 to 2.0 m, peak velocities of 3 to 7 m sec⁻¹, discharges of 25 to 250 m³ sec⁻¹ and sediment concentrations ranging from <40 wt% up to 50 to 60 wt%. Starheim *et al.* (2013) observed lahars with infrequent (>7 min intervals) high-magnitude surges which were recognised by rapid increase in flow width or depth, and more frequent (<2 min) low-magnitude pulses recognised by passing wave fronts. Froude *et al.* (2013) observed similar discharge variations on Montserrat. Extremely rapid variation in flow has also been observed in rain-triggered flash floods in the Southern Judean Desert, Israel (Cohen & Laronne, 2005; Alexandrov *et al.*, 2007), where bedload transport rates are very high in comparison with the discharge and bed shear stress. The above situations motivate some of the worked examples below.

The principal theoretical idea of the present paper can be explained as follows. From the viewpoint of a boulder moving with the spatially averaged velocity of the flow, there are fluctuations in the speed of the nearby fluid that may occur on a time scale of less than one second. These fluctuations (in space and time) of the velocity field coincide with fluctuations in the spatial gradient in pressure. When pressure differences occur over distances less than or equal to the diameter of the boulder, they are significant. This pressure difference brings about a temporary net force in the direction of the pressure-gradient. The force is directed from the high-pressure side of the boulder towards the low-pressure side. This force is referred to as the *impulsive force* herein. The field of pressure, expressed as a function of position, is

distorted by the *presence* of the boulder and modified by its *acceleration*. The distortion can make the pressure difference across the boulder greater than would occur if the boulder were absent. For a boulder at rest on the bed, large accelerations in the flow occur at the arrival of a flash flood front and with the subsequent velocity fluctuations. These accelerations exert large impulsive forces on the boulder.

The next section of this paper describes the various forces on a boulder, and highlights the relative importance of the impulsive force due to the fluid pressure fluctuations, especially at the flood front. In the following section of the paper, the critical conditions in which boulder movement might occur (from an initial state of rest on the bed) are identified. Expressions for the various forces acting on the boulder and an equation for the total force are derived. These expressions are made dimensionless to help the discussion of the important dimensionless ratios in the model, and to identify the relative importance of the several terms in various regimes of flow and boulder size. The implications for flash floods are described by presenting numerical examples, relevant to realistic situations.

FLUID FORCES ACTING ON A BOULDER ON THE BED AND AN INTRODUCTION TO THE CONCEPT OF ADDED-MASS

Figure 3A shows a simple line drawing of a boulder on the bed of a flow in steady flow con-

ditions. There is a spatially averaged flow velocity in the downslope direction, of magnitude u_0 which is independent of time. The boulder is subjected to gravity, buoyancy, the drag force, lift and the frictional resistance of the boulder to motion.

Considering unsteady flow conditions, Fig. 3B is like Fig. 3A but the fluid velocity in the downslope direction varies in time, with magnitude $u(t) = u_0 + u_1(t)$. For a body in vacuo, Newton's second law says that the net force F , equals mass times acceleration $F = ma$, where m is the inertial mass of the body. However, if the body is immersed in fluid, the force must also accelerate the fluid, especially near the body. The extra inertia, associated with the accelerating fluid, is called the *added-mass*, M_a . This added-mass is so-called because it must be added to the inertial mass, m , of the boulder. (Added-mass is a long-established concept in fluid dynamics; Paterson, 1983.)

Herein, this idea is turned around to argue that an accelerating fluid causes a force (here called the *impulsive force*) on a body in the flow. In particular, this paper considers the moving water in a flash flood suddenly encountering a boulder that is initially at rest on the bed. Near the boulder the fluid decelerates due to the impact with the boulder and this deceleration depends on position relative to the boulder. The deceleration is small far from the boulder and largest adjacent to it. Everywhere in the fluid domain there is some loss of momentum: most within a few radii of the boulder and

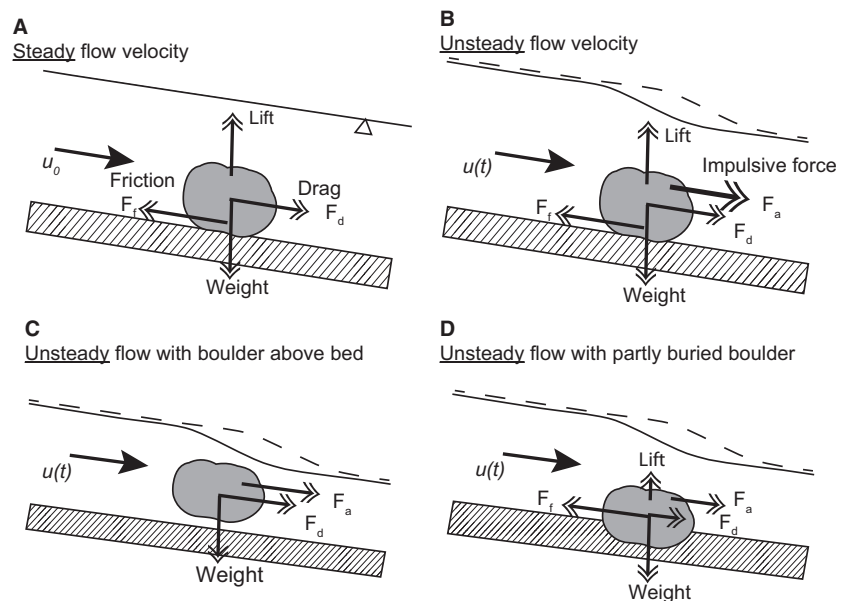


Fig. 3. Simple sketches of forces acting on a boulder in different settings. The top lines in each drawing represent the instantaneous position of the moving water surface. (A) Forces of drag F_d and friction F_f on a boulder in steady water flow. (B) The forces on the same boulder in a flow that has a rapidly changing velocity, including the impulsive force F_a . (C) Sketch of the position of a boulder above the bed with neither friction nor lift. (D) Forces on a partly buried boulder.

less further away. Newton's second law equates the associated total loss of fluid momentum (across the fluid domain) with a force, this is the *impulsive force* exerted by the fluid on the boulder.

To account for the changes in momentum throughout the fluid domain (everywhere, from the surface of the boulder out to the most distant parts of the fluid domain), requires the solution of the Laplace partial differential equation, with appropriate boundary conditions on the surface of the boulder, the bed and the water surface, together with a far-field condition (that the influence of the boulder tends to zero there). One outcome of this calculation of the field of momentum loss, is the *added-mass* of the boulder in that setting. The magnitude of M_a is directly proportional to both the fluid density ρ_f and the volume of the boulder V . Therefore $M_a = k \rho_f V$, where k is a dimensionless number that only depends on the shape and orientation of the boulder. In this paper the added-mass is estimated from values for a sphere (for which $k = 1/2$) and a vertical cylinder ($k = 1$), and the geometrical complexities of an uneven bed, neighbouring boulders or free-surface boundaries are neglected.

A way to express the *impulsive force* mathematically is to set it equal to the following product: the acceleration of the fluid (at the location of the boulder) multiplied by the added-mass, M_a . Similarly, the impulse on the boulder (the large impulsive force times its small duration) is the velocity scale of the flow multiplied by the added-mass, M_a .

Returning to Fig. 3B, in which the fluid velocity in the downslope direction varies in time, with magnitude $u(t) = u_0 + u_1(t)$, the impulsive force on the boulder can be written as $F_a(t) = M_a \times a(t)$, where M_a is the *added-mass* of the boulder, and the acceleration $a(t)$ is the time-derivative of the relative velocity $u_r = u(t) - u_s(t)$, and is associated with the rate of change in time of the velocity fluctuation relative to the (possibly moving) boulder, and where $u_s(t)$ is the velocity of the boulder relative to the bed. For a boulder at rest on the bed, $u_s(t) = 0$.

Forces acting on a boulder on the bed in a very unsteady flow

There are special conditions of flow at the front of a flash flood, or in association with a bore during a flood. The initial impact of a flood front or bore gives a short-duration but large impulsive

force, F_a , which may be big enough to overcome friction and start the boulder moving. The changes to the velocity field of the water close to the boulder during flood front or bore impact have not previously been included in theories of sediment entrainment. The special flow conditions during impact may enhance scouring under a boulder and so separate it from the bed. Any lift may also promote separation of the boulder from the bed. The impulsive force and the drag force are both important for keeping the boulder moving. The moving boulder contributes to the sediment load in the front of the flash flood and may help displace other boulders.

In a flash flood the fluid velocity $u(t)$ incident on one boulder fluctuates in time, t . Let $u_r(t) = u(t) - u_s(t)$ be the flow velocity relative to the boulder, which has velocity $u_s(t)$ relative to the bed. Apart from the drag force F_d , which is directly proportional to $u_r(t)^2$, there is also the impulsive force $F_a = M_a \times a(t)$, where M_a is the *added-mass* of the boulder (explained above) and $a(t)$ is the rate of change of $u_r(t)$. If the fluid velocity $u(t)$ suddenly changes then $a(t)$ can be briefly huge, so that F_a is a huge force that acts impulsively (over the very short time of change in the flow). The impulsive force, F_a , can briefly be much greater in magnitude than either the bed-boulder friction or the buoyant weight ($(\rho_s - \rho_f)Vg$ where ρ_f is the density of the fluid, ρ_s is the density of the boulder and V is the volume of the boulder). Like the drag force, the impulsive force is a vector quantity and acts in the same direction as the fluid acceleration (usually upstream or downstream). In a flash flood the instantaneous fluid acceleration can be temporarily in any direction in three dimensions, and not necessarily parallel to the fluid velocity. The direction of the vector F_a can change quickly, rocking the boulder out of position. The drag is directly proportional to the projected cross-section area at right angles to the time-averaged velocity of flow. Unlike drag, F_a is directly proportional to the *volume* of the boulder, via the *added-mass* M_a . The buoyant weight and friction forces are also directly proportional to the volume of the boulder. When a boulder is mobile and moving with the same speed as the flood water $F_d = 0$, but F_a can continue to act, especially if the boulder is caught up in the violently changing flow in the flash flood front.

Figure 3 illustrates the following three broad scenarios for *in situ* boulder positions. Firstly, for a blunt body, such as a near-spherical boulder sitting on a flat bed, the lift force has the

same dependence on velocity as the drag, but it is multiplied by a lift coefficient, C_l , which is generally much smaller than the drag coefficient, C_d . Secondly, most boulders are not aerodynamic shapes and a typical boulder experiences zero lift when it is above the bed and surrounded by fluid. This is because the flows over and under the boulder are similar. In an extreme situation, if the boulder is in point-contact with a plane bed then the flow under the boulder is only a little slower (with slightly higher pressures) than the flow over the boulder. This difference in pressures gives a net lift that is small compared with drag. Thirdly, in situations where the boulder is partly buried, so that only its upper surface is exposed, there is a lift due to the (lowered) pressure of the flow speeding over its top (Carling *et al.*, 2002a,b). Under these conditions the lift is likely to be similar in magnitude to the drag, until the boulder moves and flow can go under the boulder. Thereafter the lift reduces to zero. Compared to the *impulse force*, the flow front *lift* is likely to be very small.

Mathematical model of forces on the boulder

The above description is presented as a mathematical model in Fig. 3B with resolved vectors so that the components are positive in the down-slope direction for the forces, the flow velocity $u(t)$, the velocity of the boulder $u_s(t)$ and the acceleration $a(t)$. Relative to a frame fixed to the bed, Newton's second law of motion is $F = m_s \times du_s/dt$, where F is the net force on the boulder, and the boulder has inertial mass m_s and velocity $u_s(t)$. The force F is the sum of the drag, F_d , and the impulsive force, F_a , and minus the frictional force, F_f , between the boulder and the bed:

$$F = F_d + F_a - F_f \quad (1)$$

The drag $F_d = \frac{1}{2} C_d A \rho_f (u_0 - u_s)^2$, where $C_d = 1$ is the drag coefficient for a blunt body, A is the cross-sectional area of the boulder in the plane perpendicular to the flow, ρ_f is the density of the fluid, and ρ_s is the density of the boulder. The impulsive force $F_a = k \rho_f V a(t)$, where $k\rho_f V$ is the added-mass M_a , k is a dimensionless constant that depends on the shape of the boulder ($k = \frac{1}{2}$ for a sphere, $k = 1$ for a cylinder with a vertically orientated axis) and V is the volume of the boulder. The frictional force between the bed and the boulder is $F_f = \lambda (\rho_s - \rho_f) Vg$, where λ is the coefficient of friction, and $(\rho_s - \rho_f)Vg$ is the buoyant weight. These expressions, substituted

into Eq. 1, lead to the following equation for the total force F on the boulder:

$$F = \frac{1}{2} \rho_f A [u_0 - u_s(t)]^2 + k \rho_f V a(t) - \lambda (\rho_s - \rho_f) Vg \quad (2)$$

By dividing Eq. 2 by the buoyancy force the equation can be expressed in dimensionless form:

$$\frac{F}{\rho_f Vg} = \frac{1}{2Lg} [u_0 - u_s(t)]^2 + k \frac{a(t)}{g} - \lambda \left(\frac{\rho_s}{\rho_f} - 1 \right), \quad (3)$$

where the value, L , defined $L = V/A$ is a length associated with the boulder and its orientation, discussed below. When the boulder is at rest $u_s = 0$ and $F = 0$ in Eq. 2. While the boulder is stationary, the frictional force F_f increases with the applied force to an upper limit, when it moves; accordingly the friction coefficient λ lies within a restricted range: $0 < \lambda < \lambda_{\max}$ (French, 1971). Hence, for the boulder to be on the brink of moving, Eq. 2 implies $F > 0$, which in turn implies:

$$u_0^2 \geq 2Lg \left(\left(\frac{\rho_s}{\rho_f} - 1 \right) \lambda_{\max} - k \frac{a}{g} \right) \quad (4)$$

This too can be written in dimensionless terms: by dividing through Eq. 4 by gh , where h is the depth of water, so that the left-hand side is a Froude number. The criterion for boulder movement is now:

$$\frac{u_0^2}{gh} \geq 2 \frac{L}{h} \left(\left(\frac{\rho_s}{\rho_f} - 1 \right) \lambda_{\max} - k \frac{a}{g} \right) \quad (5)$$

In a flash flood the Froude number, Fr is generally expected to be about one (i.e. near critical value between tranquil and rapid flow). In natural water flows over non-cohesive mobile beds, the value of Fr rarely increases much above critical (i.e. 1) (Grant, 1997). With engineered structures (for example, weirs and dams), or in bedrock channels higher Froude numbers ($Fr = 2$ to 9) will occur locally (Hager & Bremen, 1989; Chanson, 1999). In the flash flood (not in hard engineered structures or bedrock channels) the Froude number in the flood front is higher, but not expected to exceed two (Chanson, 1999). In water of depth h it is expected that $u_0^2 = gh$, so that the left-hand side of Eq. 5 is one. Equation 5 can then be rearranged to identify the

range of sizes of boulders that are moved, as a function of fluid acceleration:

$$0 \leq L \leq \frac{hFr}{2\left(\left(\frac{\rho_s}{\rho_f} - 1\right)\lambda_{\max} - k\frac{a}{g}\right)}. \quad (6)$$

In Eq. 6 a/g is assumed to be small enough that the right-hand side (RHS) is a positive quantity. In a steady velocity field the fluid acceleration is zero, and the RHS of Eq. 6 is at its smallest, and only a limited range of boulder sizes can be moved. In an unsteady flow, as a/g is increased from zero, the denominator on RHS Eq. 6 decreases, so that the value of the fraction increases, and with it the range of mobile boulder sizes L increases.

After the motion starts the subsequent velocity $u_s(t)$, of the boulder is governed by the differential Eq. 2 with the left-hand side replaced by $m_s \times du_s/dt$, where $m_s = \rho_s V$, is the inertial mass of the boulder (different from the added-mass $M_a = k\rho_f V$). This paper concentrates on the onset of motion (initial boulder entrainment) and not the subsequent movement.

For the boulder to start moving, $F > 0$. Expression 3 contains two distinctive dimensionless ratios, each of which influences the ability of the flow to move the boulder. These ratios also appear in Eq. 6. Firstly, the ratio $(\rho_s - \rho_f)/\rho_f$ decreases as the fluid density ρ_f increases towards the (greater) density ρ_s of the boulder – as this ratio decreases, the fluid gives a bigger impulsive force to the boulder, as shown in Eq. 3. Secondly, the scaled impulsive-force term is directly proportional to the ratio of fluid acceleration, $a(t)$, to gravitational acceleration, g . As $a(t)/g$ increases, the impulsive force kicks the boulder harder. Unlike the other factors, $a(t)/g$ can change sign – it is large and positive when the flow speed suddenly increases, but negative while the fluid slows down. Remembering that the fluid acceleration vector field has components other than downstream, the impulsive force may act on the boulder in a direction quite different from the drag pushing it downstream. To illustrate how this theory works in practice some numerical examples are explored below.

IMPLICATIONS FOR FLASH FLOODS

Definite predictions can be made from the above formulae, shown here by three sample calculations.

Example 1: Assume a value for the water depth, $h = 1.6$ m, with an associated mean velocity for the flash flood front flow of $u_0 = 4$ m sec⁻¹ (in accord with Froude scaling, $u_0 = (gh)^{1/2}$ and $Fr = 1$). One choice of a maximum size of velocity fluctuations is $u_1 = 4$ m sec⁻¹. A plausible time scale over which u_1 changes is $T = 0.1$ sec. This gives an estimate for acceleration up to $a(t) = u_1(t)/T = 40$ m sec⁻². Hence $a(t)$ can have a magnitude between $0 g$ and $4 g$. To remain within the range of validity of Expression 6 the acceleration a must be between $0 g$ and $3 g$. For a spherical boulder of radius r metres, $V = 4/3 \pi r^3$, $A = \pi r^2$, hence the length scale $L = 4r/3$ for all its orientations. For a sphere, $k = 1/2$, and it is assumed that $\lambda_{\max} = 1$. For clear water the, fluid has density $\rho_f = 1000$ kg m⁻³ and the boulder has density $\rho_s = 2500$ kg m⁻³. Under these conditions, Eq. 6 implies that for the boulder to be just able to move ($u_s = 0$ and $F > 0$), its diameter to depth ratio, $2r/h$, lies in the range:

$$a < \frac{2r}{h} < \frac{3gFr}{2(3g - a)} \quad (7)$$

Suppose that $Fr = 1$. If $a = 0$ (i.e. the flow is steady), then $0 < 2r/h < 1/2$. Hence boulders of diameter ($2r$) up to one half of the depth can be moved by drag alone and larger boulders remain at rest on the bed. However, if the flow is unsteady to the extent that velocity fluctuations induce accelerations of magnitude $a = g$, then $0 < 2r < 1.2$ m, which corresponds to a boulder whose diameter ($2r$) is up to three-quarters of the depth of water. This illustrates the fact that Eq. 7 implies that as the acceleration a increases towards $3 g$, boulders are moved which have a much wider range of diameter, $2r$. If $a = 3 g/2$ then Eq. 7 suggests that all of the boulders that are submerged ($2r/h < 1$) move, because even without the drag force, the acceleration kick alone is great enough to move them. If a value of $Fr > 1$ is taken, an even wider range of boulder sizes can be expected to move, as predicted by Eq. 7.

Example 2: Another way to portray the situation with a spherical boulder in a broader context of flows, is to make a map of those combinations of u_0 and r (hence diameter $2r$) for which the boulder moves. Equation 4 implies that a boulder of radius r , in a flow of speed u_0 , moves provided:

$$u_0 \geq \left(\frac{4}{3} r(3g - a) \right)^{1/2} \quad (8)$$

In Eq. 8 the larger the value of a , the smaller the value of u_0 needed to move the boulder. This dependence is shown in Fig. 4 where dimensionless speed $u_0/(gh)^{1/2}$ is plotted as a function of dimensionless radius r/h , for several values of a . The top curve in the figure is for the traditional calculation with drag alone and $a = 0$ g. Above this curve, there is boulder movement, and below it there is no movement. As the magnitude of $a(t)$ increases, the curve moves downward, towards the horizontal axis, and reaches it when $a = 3$ g. Figure 4 can be used to infer a range of flow speeds from the observed maximum radius of moved boulders in the rock record.

A key finding of this paper is that with the inclusion of the acceleration term $a(t)$ in the model Eqs 2 to 6, the inferred flow speed u_0 may be much less than that predicted by the traditional calculation with $a = 0$ g (steady flow). For example, if $r = 0.8$ m, so that the boulder is just submerged in a depth $h = 1.6$ m, then the traditional calculation ($a = 0$ g) estimates $u_0 = 5.6$ m sec⁻¹, which is faster than a flow speed of 4.0 m sec⁻¹ based on a Froude number of one, in this depth of water; whereas, if $a = 2$ g, then the estimated flow speed is reduced to $u_0 = 3.2$ m sec⁻¹. This is a more realistic speed for this water depth, because natural flows over mobile beds tend to adjust their environment such that they are rarely much above critical Froude conditions (Grant, 1997). Although it might be argued that a flash flood may not last long enough to adjust its flow boundaries to keep Fr low, the rapid acceleration at the flow front that is capable of moving sizable particles allows boundary adjustment much faster than can occur in steady flow.

A mobile boulder moves more slowly than the fluid, so as it moves it becomes increasingly distant from the head of the flash flood front. Relative to the head the boulder moves back through the zone of flood water until it experiences either a low enough relative velocity, or shallow enough water, or a flow with small enough acceleration for bed friction to overcome the other forces. Under any one of these conditions the boulder will stop moving. A loss of impulsive force F_a or an increase in bed friction can be brought about by other factors too, including the proximity of other boulders (either moving with the flow, or at rest on the bed).

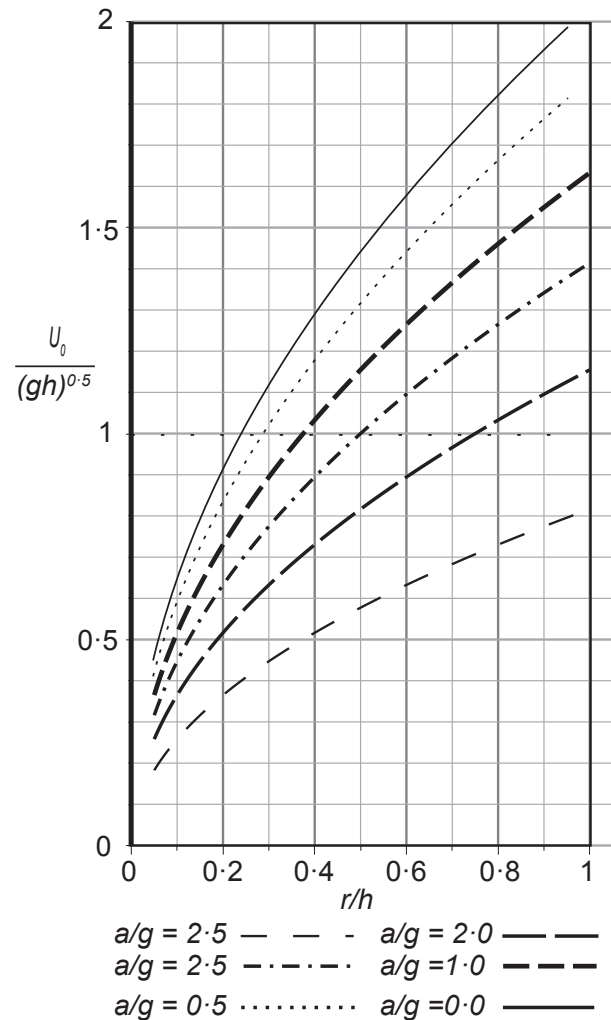


Fig. 4. The dimensionless flow speed, $u_0/(gh)^{1/2}$, as a function of dimensionless boulder radius, r/h , for several values of flow acceleration, $a/g = 0, 0.5, 1.0, 1.5, 2.0, 2.5$ (uppermost curve to lowest curve). The region above each curve corresponds to conditions of boulder movement; below the curve corresponds to no movement. The curves are truncated for small values of r , where drag dominates. The upper limit on r is the half-depth of water, to ensure that the boulder is submerged. The horizontal line $u_0/(gh)^{1/2} = 1$ corresponds to a typical upper bound on flow speed. This plot needs to be treated with caution because of the rapid variation in both h and u_0 within flash floods.

In natural flash floods the mobile sediment adds to the bulk density of the fluid, and the sediment load can vary rapidly in space and time. The density of individual boulders can differ greatly depending on composition and porosity. Also the density of the mixture can be much more than that of water. Suppose the mean density of the suspended sediment is

taken as 2500 kg m^{-3} , because it is likely to include both mineral components such as quartz and less dense particles such as organic materials. Then, for example, if the suspended sediment is: (i) 10 wt% then $\rho_f = 0.9 \times 1000 + 0.1 \times 2500 = 1150 \text{ kg m}^{-3}$; or if it is (ii) 20 wt% then $\rho_f = 0.8 \times 1000 + 0.2 \times 2500 = 1300 \text{ kg m}^{-3}$, and the density ratio in Eq. 3 decreases from 1.5 to (i) 1.17; to (ii) 0.92. Correspondingly the impulsive force in Eq. 3 becomes even more important and the dimensionless impulsive force grows by the reciprocal of the above factors, and it increases from 0.67 to (i) 0.85; to (ii) 1.08.

Example 3: The purpose of this example is to make an estimate of the range of velocities that have the capacity to move a boulder of given dimensions. The results of the present theory are compared with velocity estimates obtained by Stokes *et al.* (2012) using several methods. Stokes *et al.* (2012) report one boulder with major axes 1.1 m, 0.35 m and 0.6 m from which a geometric-mean diameter of 0.614 m is calculated. The ranges of velocity estimated by Stokes *et al.* (2012; table 4) to move this boulder (not allowing for the impulsive force introduced herein) range between 1.39 m and 3.73 m sec^{-1} from their Method 1, and 2.57 m to 5.28 m sec^{-1} from their Method 2.

An equivalent spherical boulder of diameter $2r = 0.614 \text{ m}$ and density $\rho_s = 2.3\rho_f$ (using Stokes *et al.*, 2012, assumptions of $\rho_s = 2.7 \times 10^3 \text{ kg m}^{-3}$ and $\rho_f = 1.15 \times 10^3 \text{ kg m}^{-3}$) is used for application of the present theory. From Eq. 5, to move a boulder the mean velocity u_0 and the maximum flow acceleration, a , must satisfy the inequality:

$$u_0 \geq 3.28 \left(1 - \frac{a}{2.7g} \right)^{1/2} \quad (9)$$

Depending on the value of a , in the interval zero to 2.7 g , the velocity, according to Eq. 9 may lie between zero and 3.28 m sec^{-1} . However, a large acceleration of 2.7 g is not expected to accompany a flow with zero mean velocity. Consequently a limited range for the acceleration is expected: a lies between zero and 2.5 g . In each case, the associated fluctuation time scale, $T = u_0/a$, is also calculated, where T is defined and presented in Table 1. These values of T are neither too large nor too small compared with the expected short time scales in a flash flood front.

Table 1. Values of mean velocity and duration of fluctuation estimated for a boulder subject to different flow accelerations.

a/g	u_0 (m sec^{-1})	$T = u_0/a$ (sec)
0	3.28	–
0.5	2.96	0.60
1.0	2.60	0.27
1.5	2.19	0.15
2.0	1.67	0.085
2.5	0.89	0.036

Table 2 shows the Stokes *et al.* (2012) estimated velocities (using the method of Clarke, 1996) for boulders of different sizes compared with estimates using the theory presented herein. Using as before a drag coefficient of 1, a coefficient of friction $\lambda_{\max} = 1$, $L = 4r/3$ and the added-mass coefficient $k = 1/2$, Eq. 4 implies:

$$u_0 \geq (2r)^{1/2} 4.19(1 - 0.37a/g)^{1/2} \quad (10)$$

for a steady flow ($a/g = 0$) and a rapidly changing flow with $a = 2.5 \text{ g}$ (thus a range of likely velocity fluctuations). This demonstrates how the term a/g introduces a flow acceleration that sharply reduces the velocity of the flow required to move a boulder.

If the coefficient of friction λ_{\max} it taken as 0.225 (the value used by Stokes *et al.*, 2012) then instead of Eq. 10, Eq. 4 implies that:

$$u_0 \geq (2r)^{1/2} 1.141(1 - 1.6a/g)^{1/2} \quad (11)$$

In order to keep the RHS positive a $< 0.63 \text{ g}$ and a 0.5 g is assumed in columns 5 and 6 of Table 2. The range of flow speeds estimated from the present theory is considerably less than those estimated by Stokes *et al.* (2012). Unlike the Stokes *et al.* (2012) estimates, no lift force is needed to reduce the forces of resistance.

DISCUSSION OF OTHER FACTORS TO BE CONSIDERED WHEN MODELLING BOULDER MOVEMENT

Any estimate of flow conditions from the grain size of the deposits makes the considerable assumption that all sizes of grains are available for transport. In many settings where flash floods occur the flow may be able to move larger clasts than are available for transport. Consequently the size distribution in the deposits will

Table 2. Estimated velocities (u_0) that would initiate movement of boulders of differing sizes comparing estimates from Stokes *et al.* (2012) using the Clarke (1996) method with friction coefficient $\lambda_{\max} = 0.225$ with estimates using the theory presented in this paper for steady and rapidly changing flow.

Maximum boulder size $2r$ (m)	u_0 (m sec ⁻¹) from Stokes <i>et al.</i> (2012) estimated using the Clarke (1996) method with friction coefficient $\lambda_{\max} = 0.225$	$u_{0 \max}$ (m sec ⁻¹) estimated		$u_{0 \max}$ (m sec ⁻¹) estimated with $a = 0$ and $\lambda_{\max} = 0.225$ (as used by Stokes <i>et al.</i> , 2012)		$u_{0 \min}$ (m s ⁻¹) estimated with $a = 0.5 g$ $\lambda_{\max} = 0.225$
		with $a = 0$ and $\lambda_{\max} = 1$	$u_{0 \min}$ (m sec ⁻¹) estimated with $a = 0.5 g$ $\lambda_{\max} = 1$			
0.30	1.03	2.29	0.59	0.77	0.33	
0.38	0.92	2.58	0.67	0.87	0.37	
0.46	1.17	2.84	0.73	0.96	0.41	
0.48	1.07	2.90	0.75	0.98	0.42	
0.76	1.27	3.65	0.95	1.23	0.52	
0.77	1.46	3.67	0.96	1.24	0.53	
1.00	1.49	4.19	1.09	1.41	0.60	
1.10	1.61	4.39	1.14	1.48	0.63	
1.25	1.47	4.68	1.22	1.58	0.67	
1.25	1.63	4.68	1.22	1.58	0.67	
2.50	2.54	6.62	1.72	2.23	0.95	
3.30	2.46	7.61	1.98	2.56	1.09	

Comparison of Stokes *et al.* (2012) estimated u_0 and estimates for steady flow in column 5 differ due to their appeal to lift coefficient $C_l = 0.2$ which indirectly reduces their frictional force. Column 6 demonstrates that even with a small $a = 0.5 g$ the estimated speed for initiation of boulder movement is more than halved. With $\lambda_{\max} = 0.225$, the $a \leq 0.61 g$ therefore arbitrarily $a = 0.5 g$ in columns 4 and 6.

not be representative of the flow conditions. Any estimate of flow conditions based on boulder size should consider the sediment source characteristics and palaeohydraulic reconstructions based on boulder size (if correctly calculated, taking into account all forces) should be regarded as minima.

Although published studies attempted to consider both the fluid bulk density (including sediment load; e.g. Billi, 2011) and boulder density (e.g. Clarke, 1996), the analysis herein shows that it is the fluid bulk density and the volume of the boulder that are directly proportional to the magnitude of the impulsive force. The greater the fluid bulk density (i.e. the sediment concentration and its density) and the bigger the boulder, the greater will be the kick to the boulder from the impulsive force. However, the force needed to move a particle is directly proportional to its mass, so that the ratio of fluid bulk density to boulder density must be considered.

There are very few published data on bulk density of fluid in the head of flash floods because of the extreme practical difficulty in obtaining such data. What data there are suggest that there might be rapid changes in space (for example, with height above the bed) and time (e.g. Alexandrov *et al.*, 2007; Malmon *et al.*, 2007; Gao *et al.*,

2013). Reliable data are difficult to obtain because of the occurrence of flash floods, rapid rate of change, energetics and also high suspended sediment loads exceeding measurement ranges for turbidity meters (e.g. Ziegler *et al.*, 2014). This lack of reliable data increases the value of theoretical studies of the type presented herein. Published data on suspended sediment concentration during flash floods demonstrate very wide variation between events, even within individual catchments (e.g. Alexandrov *et al.*, 2007; Francke *et al.*, 2008; Gao *et al.*, 2013; Ziegler *et al.*, 2014) and considerable scatter around predicted values from transport equations (cf. Alexandrov *et al.*, 2007; Gao *et al.*, 2013). Several attempts have been made to assess flow bulk density in lahars, using, for example, direct bucket sampling methods (Doyle *et al.*, 2011): at these high sediment concentrations and with the methods deployed the data are inherently imprecise, but do illustrate sediment concentrations over wide ranges up to and exceeding 40 wt% sediment.

In a flow, when one or more boulders are set in motion (rocking in place or moving over the bed) there will be rapid local changes in flow around each moving boulder that will increase the likelihood of other particles being entrained, irrespective of any added forcing caused by

boulders colliding with sediment in the bed. Scour of sediment around a boulder changes its exposure to the flow and may also cause it to rotate (for example, tipping upstream into a scour, cf. Fahnestock & Haushild, 1962) changing the cross-sectional area perpendicular to the flow.

In many flash flood settings, boulders may be totally emergent before the event (in the extreme case, resting on a dry bed), and remain partly emergent above the water surface throughout the event. Shvidchenko & Pender (2000) and Carling *et al.* (2002b) considered some aspects of clast emergence for mobility. In these settings, *lift* is negligible, but the *impulsive force* may be instantaneously the dominant force. Boulders have been observed rolling in flash floods that are considerably shallower than their diameter, in several settings, and this phenomenon deserves far more research.

The model presented here is about conditions local to one boulder, but in a single flash flood the flow conditions vary with location, for example there are differences across the width of a river bed. During the passage of a flood front the forces acting on particles on the bed will be much more violent at the banks where velocity magnitude and direction can vary greatly (due to enhanced wave breaking and splashes caused by shoaling water at the banks). Forces due to drag alone, in steady flow conditions, are present all the time; the much bigger impulsive force dominates under transient accelerated-flow conditions at the flash flood front, and even more so at the banks. Once the rate of change slows (when the flood front has passed) and flow becomes steadier, the entraining forces on particles are likely to be greatest away from the banks.

The short duration of a flash flood tends to generate relatively short boulder transport paths so it is likely that boulders are not buried in the waning phase of the flood (as in Fig. 2B). The consequence of this is that in the rock record, a boulder may be surrounded mostly by sediment deposited by later events. In this case, when interpreting depositional history, it is essential to establish which bed was deposited with the boulder being considered.

CONCLUSIONS

The above theory shows that in flash floods, where flow conditions vary rapidly: (i) the impulsive force can help the drag force to impel boulders

into motion; (ii) the estimate of flow speed that moves a given maximum size of boulder is greatly reduced if the impulsive force is included; (iii) for larger boulders (up to the depth of water) the impulsive force can be greater than the drag force; and (iv) the impulsive force may act in any direction, including upstream for the short time it acts and the vector F_a can change quickly, rocking the boulder out of position.

ACKNOWLEDGMENTS

The authors are grateful to Paola Billi, Paul Carling, Melanie Froude, Vern Manville and Anne Mather for constructive comments on early drafts of this paper. We also thank Anne Mather and Mel Froude for letting us use the photographs in Fig. 2.

NOMENCLATURE

A	Cross-sectional area of the boulder in plane perpendicular to the flow direction
A	Acceleration
$a(t)$	Rate of change of $u_r(t)$. The time-derivative of the relative velocity $u_r = u(t) - u_s(t)$, associated with the rate of change in time of the fluid velocity fluctuation relative to the boulder
C_l	Lift coefficient
C_d	Drag coefficient. $C_d = 1$ for a blunt body
F	Force
$F_a(t)$	Impulsive force $F_a(t) = M_a \times a(t)$
F_d	Drag force
F_f	Frictional force
Fr	Froude number
g	Acceleration due to gravity, $g = 9.8 \text{ m sec}^{-2}$
h	The water depth
k	Dimensionless coefficient of added-mass, Depends on the shape of the boulder
L	Defined $L = V/A$ is a length associated with the boulder and its orientation
M	The inertial mass of a boulder
M_a	Added-mass of the boulder
R	Radius of a boulder ($2r$ is diameter)
T	An interval of time over which the velocity fluctuates

U	Streamwise fluid velocity
$u(t)$	Magnitude of fluid velocity, varying in time, in a downslope direction = $u_0 + u_1(t)$
u_0	Time-averaged fluid velocity
$u_1(t)$	Fluctuations in the fluid velocity
$u_r(t)$	Fluid velocity measured relative to the boulder
$u_s(t)$	Velocity of the boulder. For a boulder at rest on the bed $u_s(t) = 0$
V	Volume of the boulder
ρ_f	Density of the fluid
ρ_s	Density of the boulder
λ	The coefficient of friction: a dimensionless parameter describing resistance to flow exerted by an obstacle on the bed
λ_{\max}	Maximum value of λ

REFERENCES

- Alexander, J., Barclay, J., Sušnik, J., Loughlin, S.C., Herd, R.A., Darnell, A. and Croswell, S. (2010) Sediment-charged flash floods on Montserrat: the influence of synchronous tephra fall and varying extent of vegetation damage. *J. Volcanol. Geoth. Res.*, **194**, 127–138.
- Alexandrov, Y., Laronne, J.B. and Reid, I. (2007) Intra-event and inter-seasonal behaviour of suspended sediment in flash floods of the semi-arid northern Negev, Israel. *Geomorphology*, **85**, 85–97.
- Alho, P., Baker, V.R. and Smith, L.N. (2010) Paleohydraulic reconstruction of the largest Glacial Lake Missoula draining(s). *Quatern. Sci. Rev.*, **29**, 3067–3078.
- Andrews, E.D. (1983) Entrainment of gravel from naturally sorted riverbed material. *Geol. Soc. Am. Bull.*, **94**, 1225–1231.
- Archer, D.R. and Fowler, H.J. (2015) Characterising flash flood response to intense rainfall and impacts using historical information and gauged data in Britain. *J. Flood Risk Manage.*, 1–13. doi:10.1111/jfr3.12187.
- Barclay, J., Alexander, J. and Sušnik, J. (2007) Rainfall-induced lahars in the Belham valley, Montserrat, West Indies. *J. Geol. Soc. London*, **164**, 815–827.
- Billi, P. (2011) Flash flood sediment transport in a steep sand-bed ephemeral stream. *Int. J. Sed. Res.*, **26**, 193–209.
- Bohorquez, P. (2008) On the wave-front shape and the advancing of the wetting front of a dam-break flood over an inclined plane of arbitrary bottom slope. In: *Proceedings of the International Workshop on Numerical Modelling of Hydrodynamics for Water Resources – Numerical Modelling of Hydrodynamics for Water Resources* (Ed. P. Garcia-Navarro and E. Playan), pp. 355–359. Taylor & Francis, London.
- Bridge, J.S. and Bennett, S.J. (1992) A model for the entrainment and transport of sediment grains of mixed sizes, shapes and densities. *Water Resour. Res.*, **28**, 337–363.
- Carling, P.A., Hoffmann, M., Blatter, A.S. and Dittrich, A. (2002a) Drag of emergent and submerged rectangular obstacles in turbulent flow above bedrock surface. In: *Rock Scour Due to Falling High-Velocity Jets* (Eds A. Schleiss and E. Bollaert), pp. 83–94. Swets & Zeitlinger, Lisse.
- Carling, P.A., Hoffmann, M. and Blatter, A.S. (2002b) Initial motion of boulders in bedrock channels. In: *Ancient Floods, Modern Hazards: Principles and Application of Paleoflood Hydrology* (Eds. P. Kyle House, R.H. Webb, V.R. Baker & D.R. Levish), *Water Sci. Appl.*, **5**, 147–160.
- Carrivick, J.L. (2007) Modelling coupled hydraulics and sediment transport of a high-magnitude flood and associated landscape change. *Ann. Glaciol.*, **45**, 143–154.
- Carrivick, J.L., Manville, V. and Cronin, S.J. (2009) A fluid dynamics approach to modelling the 18th March 2007 lahar at Mt. Ruapehu, New Zealand. *Bull. Volcanol.*, **71**, 153–169.
- Carrivick, J.L., Manville, V., Graettinger, A.H. and Cronin, S.J. (2010) Coupled fluid dynamics-sediment transport modelling of a Crater Lake break-out lahar: Mt. Ruapehu, New Zealand. *J. Hydrol.*, **388**, 399–413.
- Chanson, H. (1999) *The Hydraulics of Open Channel Flow*. Heinemann, Butterworth, 544 pp.
- Church, M. (1978) Paleohydrological reconstructions from a Holocene valley fill. In: *Fluvial Sedimentology* (Ed. A.D. Miall), *Can. Soc. Petrol. Geol. Mem.*, **5**, 743–772.
- Church, M., Hassan, M.A. and Wolcott, J.F. (1998) Stabilizing self-organized structures in gravel-bed stream channels: field and experimental observations. *Water Resour. Res.*, **34**, 3169–3179.
- Clarke, A.O. (1996) Estimating probable maximum floods in the Upper Santa Ana Basin, Southern California, from stream boulder size. *Environ. Eng. Geosci.*, **2**, 165–182.
- Cohen, H. and Laronne, J.B. (2005) High rates of sediment transport by flash floods in the Southern Judean Desert, Israel. *Hydrol. Process.*, **19**, 1687–1702.
- Cooker, M.J. and Peregrine, D.H. (1995) Pressure impulse theory for liquid impact problems. *J. Fluid Mech.*, **297**, 193–214.
- Cornish, V. (1910) *Waves of the Sea and Other Water Waves*. Fisher T. Unwin, London, 367 pp.
- Costa, J.E. (1983) Paleohydraulic reconstruction of flash-flood peaks from boulder deposits in the Colorado Front Range. *Geol. Soc. Am. Bull.*, **94**, 986–1004.
- Cox, S.J. and Cooker, M.J. (1999) The motion of a rigid body impelled by sea-wave impact. *Appl. Ocean Res.*, **21**, 113–125.
- Cronin, S.J., Neall, V.E., Lecointre, J.A. and Palmer, A.S. (1997) Changes in Whangaehu River lahar characteristics during the 1995 eruption sequence, Ruapehu volcano, New Zealand. *J. Volcanol. Geoth. Res.*, **76**, 47–61.
- Darnell, A.R., Phillips, J.C., Barclay, J., Herd, R.A., Lovett, A.A. and Cole, P.D. (2013) Developing a simplified geographical information system approach to dilute lahar modelling for rapid hazard assessment. *Bull. Volcanol.*, **75**(4), 1–16.
- Doyle, E.E., Cronin, S.J. and Thouret, J.-C. (2011) Defining conditions for bulking and debulking in lahars. *Geol. Soc. Am. Bull.*, **123**, 1234–1246.
- Fahnestock, R.K. and Haushild, W.L. (1962) Flume studies of the transport of pebbles and cobbles on a sand bed. *Geol. Soc. Am. Bull.*, **73**, 1431–1436.
- Ferguson, R.I. (2005) Estimating critical stream power for bedload transport calculations in gravel-bed rivers. *Geomorphology*, **70**, 33–41.
- Francke, T., López-Tarazón, J.A., Vericat, D., Bronstert, A. and Batalla, R.J. (2008) Flood-based analysis of high-magnitude sediment transport using a non-parametric method. *Earth Surf. Proc. Land.*, **33**, 2064–2077. doi:10.1002/esp.1654.

- French, A.P.** (1971) *Newtonian Mechanics*. W.W. Norton and Co., New York, NY, 743 pp.
- Froude, M.J.** (2015) *Lahar dynamics in the Belham river valley, Montserrat: application of remote-camera based monitoring for improved sedimentological interpretation of post-event deposits*. Doctoral thesis, University of East Anglia.
- Froude, M.J., Alexander, J., Barclay, J. and Cole, P.D.** (2013) Multi-order discharge fluctuations in lahars in the Belham Valley, Montserrat. International Conference on Fluvial Sedimentology, abstract volume, International Association of Sedimentologists.
- Gao, P., Nearing, M.A. and Commons, M.** (2013) Suspended sediment transport at the instantaneous and event time scales in semiarid watersheds of southeastern Arizona, USA. *Water Resour. Res.*, **49**, 6857–6870. doi:10.1002/wrcr.20549.
- Graf, W.H.** (1971) *Hydraulics of Sediment Transport*. McGraw-Hill Book Co., New York, NY, 513 pp.
- Grant, G.E.** (1997) Critical flow constrains flow hydraulics in mobile-bed streams: a new hypothesis. *Water Resour. Res.*, **33**, 349–358.
- Hager, W.H. and Bremen, R.** (1989) Classical hydraulic jump: sequent depths. *J. Hydraul. Res.*, **27**, 565–585.
- Hjalmarson, H.W.** (1984) Flash flood in Tanque Verde Creek, Tucson, Arizona. *J. Hydraul. Eng.*, **110**, 1841–1852. doi:10.1061/(ASCE)0733-9429(1984)110:12(1841).
- Iverson, R.M.** (1997) The physics of debris flows. *Rev. Geophys.*, **35**, 245–296.
- Jasek, M.** (2003) Ice jam release surges, ice runs, and breaking fronts: field measurements, physical descriptions, and research needs. *Can. J. Civ. Eng.*, **30**, 113–127.
- Jeffreys, H.** (1925) The flow of water in an inclined channel of rectangular section. *Phil. Mag.*, **49**, 793–807.
- Kilgour, G., Manville, V., Della Pasqua, F., Rayes, A.G., Graettinger, A.H., Hodgson, K.A. and Jolly, A.D.** (2010) The 25 September 2007 eruption of Mt. Ruapehu, New Zealand: directed ballistics, Surtseyan jets, and ice-slurry lahars. *J. Volcanol. Geoth. Res.*, **191**, 1–14.
- Komar, P.** (1987) Selective gravel entrainment and the empirical evaluation of flow competence. *Sedimentology*, **34**, 1165–1176.
- Komar, P.** (1989) Flow-competence evaluations of the hydraulic parameters of floods: an assessment of the technique. In: *Floods: Hydrological, Sedimentological, and Geomorphological Implications* (Eds K. Beven and P. Carling), pp. 107–135. Wiley, New York.
- Komatsu, G., Arzhannikov, S.G., Gillespie, A.R., Burke, R.M., Miyamoto, H. and Baker, V.R.** (2009) Quaternary paleolake formation and cataclysmic flooding along the upper Yenisei River. *Geomorphology*, **104**, 143–164.
- Laronne, J.B. and Carson, M.A.** (1976) Interrelationships between bed morphology and bed-material transport for a small, gravel-bed channel. *Sedimentology*, **23**, 67–85.
- Lube, G., Cronin, S.J., Manville, V., Procter, J.N., Cole, S.E. and Freudt, A.** (2012) Energy growth in laharc mass flows. *Geology*, **40**, 475–478.
- Malmon, D.V., Reneau, S.L., Katzman, D., Lavine, A. and Lyman, J.** (2007) Suspended sediment transport in an ephemeral stream following wildfire. *J. Geophys. Res.*, **112**, doi:10.1029/2005JF000459.
- Mather, A.E. and Hartley, A.** (2005) Flow events on a hyper-arid alluvial fan: Quebrada Tambores, Salar de Atacama, northern Chile. In: *Alluvial Fans: Geomorphology, Sedimentology, Dynamics* (Eds A.M. Harvey, A.E. Mather and M. Stokes), *Geol. Soc. London Spec. Publ.*, **251**, 9–29.
- McComb, W.D.** (1990) *The Physics of Turbulence*. Oxford University Press, Oxford, 572 pp.
- Meirovich, L., Laronne, J.B. and Reid, I.** (1998) The variation of water-surface slope and its significance for bedload transport during floods in gravel-bed streams. *J. Hydraul. Res.*, **36**, 147–157.
- Mulder, T. and Alexander, J.** (2001) The physical character of subaqueous sedimentary density currents and their deposits. *Sedimentology*, **48**, 269–299.
- O'Connor, J.E.** (1993) Hydrology, hydraulics, and geomorphology of the Bonneville Flood. *Geol. Soc. Am. Spec. Pap.*, **274**, 1–84.
- Parker, C., Clifford, N.J. and Thorne, C.R.** (2011) Understanding the influence of slope on the threshold of coarse grain motion: revisiting critical stream power. *Geomorphology*, **126**, 51–65.
- Paterson, A.R.** (1983) *A First Course in Fluid Dynamics*. Cambridge University Press, Cambridge, 528 pp.
- Petit, F., Gob, F., Houbrechts, G. and Assani, A.A.** (2005) Critical specific stream power in gravel-bed rivers. *Geomorphology*, **69**, 92–101.
- Reid, I., Laronne, J.B. and Powell, M.D.** (1998) Flash-flood and bedload dynamics of desert gravel-bed streams. *Hydrol. Process.*, **12**, 543–557.
- Shvidchenko, A.B. and Pender, G.** (2000) Flume study of the effect of relative depth on the incipient motion of coarse uniform sediments. *Water Resour. Res.*, **36**, 619–628.
- Spinewine, B. and Zech, Y.** (2007) Small-scale laboratory dam-break waves on movable beds. *J. Hydraul. Res.*, **45**, 73–86.
- Starheim, C.C.A., Gomez, C., Davies, T., Lavigne, F. and Wassmer, P.** (2013) In-flow evolution of lahar deposits from video-imagery with implications for post-event deposit interpretation, Mount Semeru, Indonesia. *J. Volcanol. Geoth. Res.*, **256**, 96–104.
- Stokes, M., Griffiths, J.S. and Mather, A.** (2012) Palaeoflood estimates of Pleistocene coarse grained river terrace landforms (Rio Almanzo, SE Spain). *Geomorphology*, **149**, 11–26. doi:10.1016/j.geomorph.2012.01.007.
- Vallance, J.W.** (2000) Lahars. In: *Encyclopaedia of Volcanoes*, pp. 601–616. (Eds H. Sigurdsson, B.F. Houghton, S. McNutt, H. Rymer and J. Stix), Academic Press San Diego, CA.
- Vignaux, M. and Weir, G.J.** (1990) A general model for Mt Ruapehu lahars. *Bull. Volcanol.*, **52**, 381–390.
- Weir, G.J.** (1982) Kinematic wave theory for Ruapehu lahars. *NZ J. Sci.*, **25**, 197–203.
- Williams, G.P.** (1983) Paleohydrological methods and some examples from Swedish fluvial environments. I. Cobble and boulder deposits. *Geogr. Ann.*, **65A**, 227–243.
- Zanutigh, B. and Lamberti, A.** (2007) Instability and surge development in debris flows. *Rev. Geophys.*, **45**(3), Art. no. RG3006.
- Zech, Y. and Soares-Frazaõ, S.** (2007) Dam-break flow experiments and real-case data. A database from the European IMPACT research. *J. Hydraul. Res.*, **45**, 5–7.
- Ziegler, A.D., Benner, S.G., Tantasirin, C., Wood, S.H., Sutherland, R.A., Sidle, R.C., Jachowski, N., Nullet, M.A., Xi, L.X., Snidvongs, A., Giambelluca, T.W. and Fox, J.M.** (2014) Turbidity-based sediment monitoring in northern Thailand: hysteresis, variability, and uncertainty. *J. Hydrol.*, **519**, 2020–2039.

Manuscript received 23 March 2015; revision accepted 9 February 2016